Thermochimica Acta, 151 (1989) 241–259
Elsevier Science Publishers B.V., Amsterdam — Printed in The Netherlands

HEAT CAPACITY, ENTHALPY AND CRYSTALLINITY OF POLYMERS FROM DSC MEASUREMENTS AND DETERMINATION OF THE DSC PEAK BASE LINE

V.B.F. Mathot and M.F.J. Pijpers

Structure and Morphology of Materials Section, DSM Research,
P.O. Box 18, 6160 MD Geleen (The Netherlands)

SUMMARY

This article discusses the determination of heat capacities with power compensating DSC using the continuous measuring method. Important is comparison of measurement results with reference values for heat capacity and enthalpy at the extreme states the material can be in. Within the framework of the two-phase model a description is given of the calculation of transition enthalpy and enthalpy-based temperature-dependent weight crystallinity both from heat capacity measurements and ordinary, quantitative DSC measurements by means of extrapolation from the melt. Examples are given for linear polyethylene (LPE), ultra-high molecular weight polyethylene (UHMWPE), linear low density polyethylene (LLDPE) and an ethylene-propylene copolymer. In crystallization and melting, exact determination of base-line heat capacity, $c_{p_b}(T)$, and excess heat capacity, $c_{p_e}(T)$, from the measured heat capacity $cp(T) = c_{p_b}(T) + c_{p_e}(T)$ is illustrated using the example of very low density polyethylene (VLDPE). $c_{p_e}(T)$ and the base-line signal, $(dq/dt)_b$, can also be calculated for ordinary quantitative DSC measurements. The outlined procedures apply not only to polymers with ethylene crystallinity but generally to polymers to which the two-phase model is applicable and of which the enthalpy reference values are known.

INTRODUCTION

The study of the thermal properties of polymers by calorimetric methods has become widespread in the past two decades. This development started off with the increasing availability of commercial differential calorimeters. The DSC instruments currently available have in common that they are reasonably simple to operate, that sample masses have been reduced to milligram level, and that in cooling as well as in heating the scanning rate can be high (in the case of heat-flux DSC) to very high (in the case of power-compensating DSC).

Especially in the polymer field this is a major advantage because of the kinetic determinacy of all types of processes that is so characteristic of polymers. This, in combination with an accuracy sufficient for many types of polymer research has led to a still increasing popularity. The main field of application of calorimetry on polymers is the study of phase transitions and their kinetics, more in particular the study of crystallization and melting processes [1].

Though the heat capacity of a material is an extremely important thermal property, quantitative C_p measurements are seldom made although this is

004-6031/89/$03.50 © 1989 Elsevier Science Publishers B.V.

possible with a DSC within an acceptable time span. Examples of such quantitative measurements with a DSC are given in this article with, as practical application, the determination of crystallinity as a function of temperature for polymers to which the two-phase model is applicable. With the aid of crystallinity it is also possible to calculate an exact base line under a crystallization or melting peak. This is particularly useful in cases in which the phase transition extends over extremely large temperature ranges. The procedures described are also applicable in part to ordinary, non-C_p, DSC curves.

INSTRUMENTATION

The measurements were performed with a Perkin-Elmer calorimeter, type DSC-2. The block surrounding the measuring unit is thermostatted by means of a metal buffer at a temperature which, depending on the cooling rate, is set to minimally 30 °C below the lowest measuring temperature. This thermostatting takes place by means of a pulsating liquid nitrogen supply, controlled by a Cryoson model TRL5 unit. As a result, the measurements obtained are highly reproducible and stable in time. The temperature calibrations are made with the aid of very pure metals at the applied block temperatures (-120 °C and +10 °C). Dry nitrogen is used as purging gas. The sample masses are determined to the nearest µg with a Mettler ME 22/36 electronic microbalance.

The DSC is linked on-line with a Tektronix graphic computer, model 4052A, equipped with a 20 Megabyte TransEra hard-disk, a hard copy unit and a Tektronix 4662 interactive plotter. The interfacing between DSC-2 and computer consists of a Hewlett-Packard 3495A scanner, a Hewlett-Packard (3455A or 3456A) 6 1/2 digit digital voltmeter, a Hewlett-Packard 59306A relay actuator and a 59308A timing generator.

The analogue temperature signal and the measuring signal are scanned at a frequency of 20 Hz and digitalized, the circuit being short-circuited during the intervals to prevent interaction between the signals. With the chosen combination of ranges of voltmeter and DSC, a signal between -50 mW and +50 mW can be measured within 0.5 µW. Accuracy is only further limited by noise. The analogue temperature signal (0 - 8 V) is read to 0.1 mV accuracy and, in conversion to temperature, rounded off to 0.1 degree. In all dynamic measurements with scanning rates up to 20 °C/min, temperature and measuring value are stored for each 0.1 degree as a standard procedure. At higher scanning rates the temperature interval is adapted to the rate of A/D conversion. The temperature programme is also monitored with the same multiplexer/voltmeter combination. Whenever the actual temperature appears to deviate from the DSC-2 programme temperature, the system gives a warning signal and the performed measurement is not stored in the computer memory. This also

applies to a failure in the cooling unit. These safety features increase in particular the reliability of measurements made outside of normal office hours.

By means of a computer signal, the DSC-2's internal pulse generator can be replaced by an external programmable pacer (timing generator). This makes it possible to perform measurements at any arbitrary scanning rate. This rate does not have to be constant and can assume any function of e.g. time and temperature.

The 'heat', 'hold' and 'cool' functions of the DSC-2 are driven by a relay actuator incorporated into the multiplexer. An additional external relay actuator enables computer-controlled engagement and disengagement of all kinds of peripheral equipment.

The measuring programme can take a practically unlimited number of time-temperature steps. Each step, which consists of a maximum of 2000 data points (one data point = temperature + measuring value) is stored in the mass memory, together with measuring conditions. The isotherms before and after measurement are also standardly determined, if this has been incorporated into the measuring procedure. The stored measurements are processed off-line using in-house developed software.

MEASURING METHODS

The choice of the measuring range depends not only on the phenomenon to be studied but also on whether before and after the occurrence of the phenomenon isotherms can be found where the measuring signal is not influenced by any processes whatsoever while the isothermal signal is being recorded. In the study of crystallization and melting processes, on the low temperature side of the process the ideal is to take an isotherm below the glass transition, but it is often possible to take an isotherm above the glass transition, provided that it is sufficiently far removed from the peak on the temperature scale. On the high temperature side of the process an isotherm in the melting region can usually be taken. If the phenomenon studied extends into the glass transition region, it is definitely necessary to take an isotherm below the transition, a difference of a few tens of degrees being recommendable in many cases.

A common measuring procedure is to record a (first) heating curve on as-supplied material, which often provides insight into the thermal history of the sample. Next, from the 'liquid' state (here referred to as l) - which can be a molten state (m) above the melting region or a supercooled melt above the crystallization region or an amorphous state (a) above the glass transition region - the sample is cooled at a rate of choice, down to the solid state (s), which may be a crystalline state (c) or a glassy state (g). In case of crystallizable polymers the fully crystalline state is hardly ever reached, the final state being a semi-crystalline state. After this (first) cooling curve, a

(second) heating curve is recorded, revealing the effect of the thermal history imposed by the experimenter. Usually, standard temperature ranges and scanning rates are applied.

In general, DSC and DTA yield better quantitative results in heating than in cooling; the cooling curves often show a higher degree of curvature. However, this is no reason to report heating curves only, as is often done, for cooling curves are equally important, especially in the case of polymers.

Whatever high-quality measuring head is used, a certain asymmetry of sample holder and reference holder cannot be avoided, which means there will be a nett measuring signal in the absence of sample, which signal can show a certain degree of curvature across a wide temperature range. First of all, this curvature should be minimized according to the manufacturer's instructions. Further, it is recommendable to regularly store in the computer memory the curve obtained with the two empty holders or, in the case of heat capacity measurements, with the holders holding empty pans plus lids. This curve, which corresponds to what we shall term the empty pan measurement, is then subtracted from each curve taken in the same temperature range, so that the nett measuring signal has no curvature. In the case of isothermal measurements, an analogous procedure can be followed, for example to correct for phenomena caused by instrument stabilizing after reaching the measuring temperature at a high scanning rate.

The last-mentioned method is essentially already the procedure of heat capacity (C_p) measurements [2,3]. In actual C_p measurements according to the classical method, a complication arises, especially with polymers; see [4] and references therein. The usual step width of 25-30 degrees is unsuitable if during the isothermal waiting periods thermal processes take place, such as crystallization or melting, so that no stable isotherms are to be expected before or after a temperature increment and truly quantitative measurement is impossible. In such cases, the step width will have to be enlarged to, say, 100-200 degrees, and the stability of the calorimeter will have to be improved. This measuring method will be referred to as the 'continuous' method, as opposed to the 'stepwise' method.

Fig. 1 shows DSC specific heat capacity, $c_p(T)$ (specific quantities are indicated by lower-case letters), cooling curves (cc) and heating curves (hc) for sapphire (Al_2O_3) and an amorphous ethylene-propylene copolymer with 45 mole % ethylene [5]. It is clear that in heating as well as in cooling the continuous method (measurement at 10 °C/min in one step of 250 degrees in between -70 °C and 180 °C) gives results that are in fair agreement with those obtained by the stepwise method, here applied with steps of 25 degrees at a scanning rate of 10 °C/min. There is also agreement with the literature data for sapphire. At the lowest temperatures, glass transition phenomena are seen

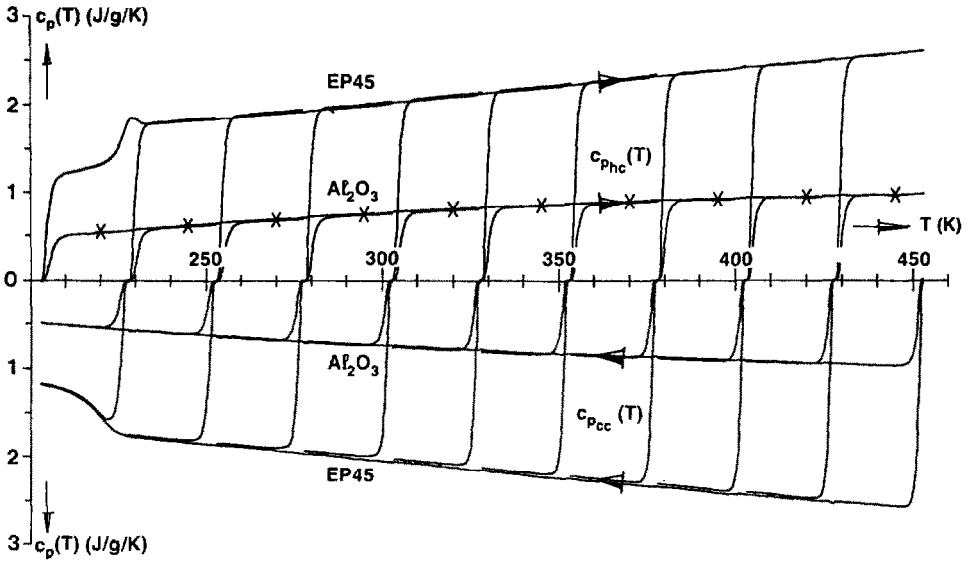

Fig. 1. DSC-2 continuous and stepwise specific heat capacity curves for cooling, $c_{p_{cc}}(T)$, and subsequent heating, $c_{p_{hc}}(T)$, for sapphire and an ethylene-propylene copolymer. X indicates literature values for sapphire.

for EP45, while the temperature dependence of c_p is strikingly linear over more than 200 degrees. The cooling and heating curves are symmetrical with respect to the temperature axis, which inspires confidence in the measurements from a thermodynamic viewpoint. It should be noted here that c_p values measured in cooling are scarce, although such measurements are at least as important as the usual c_p measurements in heating.

To preserve the link with the power-compensating DSC presentation, in the figures given here the c_p curves are plotted upwards in heating and downwards in cooling, because in heating usually endothermic processes occur and in cooling exothermic processes. Since c_p will usually be positive in both cases, the corresponding ordinates are both taken positive.

As an example of exothermic and endothermic transitions, Fig. 2 shows that LLDPE (Linear Low Density Polyethylene) covers large crystallization and melting ranges, and DSC curves of this heterogeneous ethylene-octene copolymer show several peaks [6]. By contrast, the homogeneous EP (ethylene-propylene) copolymer produces a single-peak DSC curve. DSC here functions as molecular fingerprint for copolymers with crystallizable ethylene sequences, the sequences being formed by the distribution of uncrystallizable or poorly crystallizable comonomer units in the polymer chains [7]. The figure nicely shows that even when overall quantities like density and peak area are the

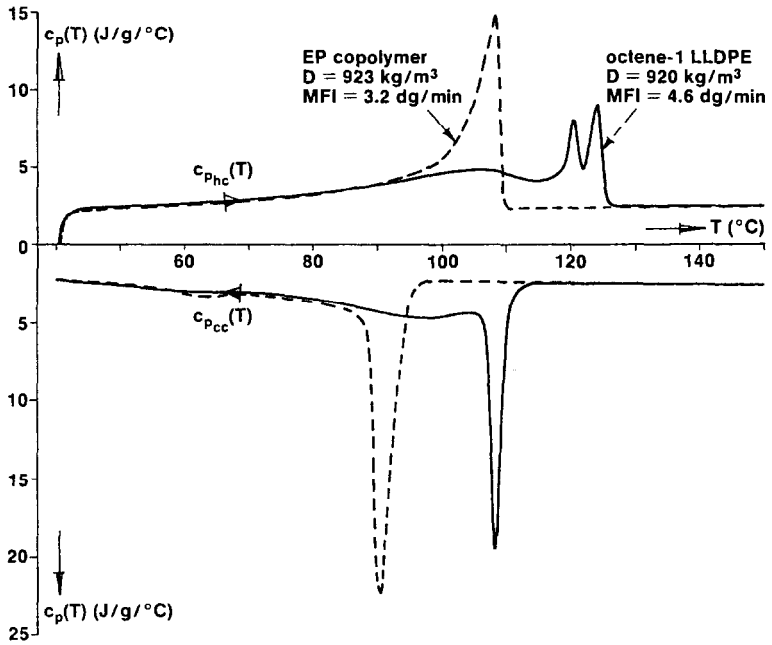

Fig. 2. DSC-2 specific heat capacity curves for cooling, $c_{P_{cc}}(T)$, at 5 °C/min from 200 °C to 40 °C and subsequent heating, $c_{P_{hc}}(T)$, at 5 °C/min. Isothermal stays of 5 min, sample masses 4.870 mg (EP) and 4.976 mg (LLDPE).

same, the crystallization and melting point distributions can be totally different.

HEAT CAPACITY

The heat capacity of a material is an extremely important thermal property. It provides direct experimental information on the possibilities of motion of the molecules and parts thereof, while quantities derived from it, e.g. enthalpy, entropy and free enthalpy, can provide important information about the state of the material. Also from a technological point of view, quantitative C_p and resulting enthalpy data are important.

The temperature dependence of the quantities [8] just mentioned is particularly important in crystallization and melting processes of semicrystalline polymers, as these often cover wide temperature ranges, and it is also a factor in the study of glass transition phenomena taking place in more or less amorphous polymers.

When a material is in the liquid state, be it either amorphous or molten, its heat capacity as a function of temperature, $c_{p_l}(T)$, is often fairly accurately approximated by a straight line over a reasonably broad temperature range [8,9].

In the case of crystallizable polymers, the heat capacity for 100 % amorphous material, $c_{p_a}(T)$, between T_g and T_m has been determined mostly via combining $c_{p_l}(T)$ data with data resulting from extrapolations according to crystallinity at intermediate temperatures using semicrystalline samples with different crystallinities, see ATHAS data bank [10]. The heat capacity for 100 % crystalline material, $c_{p_c}(T)$, has been determined in rare cases from direct measurements on such samples, but mostly via analogous extrapolations according to crystallinity.

An evaluation of the aforementioned heat capacity data [8] showed that in between T_g and T_m the heat capacity differential function, defined as $\Delta c_p(T) = c_{p_l}(T) - c_{p_s}(T)$, is a decreasing function with temperature. It has its maximum at T_g, and for crystallizable polymers it is virtually zero below T_g because there $c_{p_g} \approx c_{p_c}$.

RELATED THERMODYNAMIC FUNCTIONS

If a complete heat capacity analysis has been performed for a polymer and $c_{p_l}(T)$ and $c_{p_s}(T)$ are known, the quantities h(T), s(T) and g(T) for the liquid state and the solid state can be directly derived. The ATHAS data bank [10] contains such data on very many polymers.

These so-called reference states are of great use in the evaluation of DSC experiments on polymers, as will be illustrated here for polymers with ethylene crystallinity.

DIFFERENTIAL FUNCTIONS

As already noted, the heat capacity differential function for polymers decreases with temperature in the region between T_g and T_m. Since for polyethylene, see Table 4, ref. 8, $\Delta c_p(T_m) \approx 0$, it follows that both the enthalpy differential function, $\Delta h(T)$, and the entropy differential function, $\Delta s(T)$, reach their maxima around T_m. This means that below T_m, $\Delta h(T)$ and $\Delta s(T)$ are smaller and that, depending on the extent of supercooling ($T_m - T$), the width of the melting range, etc., the temperature dependence of the differential functions has to be taken into account in the evaluation of the measuring results. For a small extent of supercooling, $\Delta h(T) \approx \Delta h(T_m) = 293$ J/g (heat of fusion). For a large extent of supercooling, all data needed for assessment of the temperature dependence of the differential functions can be found in the Table 4, ref. 8, while in [4,8] analytical approximations for practical applications are given.

TRANSITION ENTHALPIES

In determining first order transition enthalpies, the thermal analyst is often faced with the problem where to draw the base line under the DSC-peak. He

will usually choose two points before and after the peak, connect them by a straight line and determine the area above the line. The choice of these points is rather arbitrary, although most analysts will develop a certain 'feel'.

This illustrates the need for an analyst-independent evaluation where possible. Also, more insight should be obtained into the exact nature of the quantity evaluated when a certain base line is drawn and the area above it is calculated. Further, it is necessary to know whether the heat capacity before, during and after the transition has to be corrected for and, if so, how.

Figure 2 shows how difficult peak evaluations can be. If one wants to determine a peak area in both melting curves, the problem becomes clear: which points on the curves should be connected? Extrapolation from the melt, a commonly applied procedure, in this case barely gives a point of intersection (just above 40 °C, with the portion of each curve that in part relates to the starting of the instrument), so this is no quantitative solution. In cases like this one usually just takes an (arbitrary!) point on the curve at a low temperature. Since a slight variation on the curve can considerably influence the peak area thus found, this procedure is unsatisfactory and one feels forced to extend the measuring range to lower temperatures.

In specific cases, an amorphous sample like the EP45 sample shown in Fig. 1 is used as a reference for determining the contributions of crystallization and melting to c_p in crystallizable EP samples [5]. The problem is that in most analyses such a sample serving as a 'blank' is not available. The example does show that, as such, extrapolation from the melt is a plausible method to get an approximation of $c_{p_a}(T)$, and leads to an approximation of the reference function $h_a(T)$ in the transition region. So, in fact, by extrapolating one can correct h(T) [based on the experimental $c_p(T)$], by the $h_a(T)$ profile in the temperature range in question. This procedure is useful in determining crystallinity as a function of the temperature. However, it must be realized that $c_{p_a}(T)$ does not equal the base line; this will be commented on in the last paragraph.

CRYSTALLINITY FROM DSC CURVES

If extrapolation yields a point of intersection, say at T*, it results in a peak area for the heating curve, denoted by $A_{1,hc,T*}$, see Fig. 3. Cooling curves are treated in an analogous manner.

For polymers, usually a two-phase model is assumed in which the polymer is considered to be made up of phases which have a purely amorphous or purely crystalline character, while additivity is assumed of a number of properties of the phases. In crystallization/melting the crystallinity can be defined in such a model as the relative amount of material that exists in the purely crystalline state.

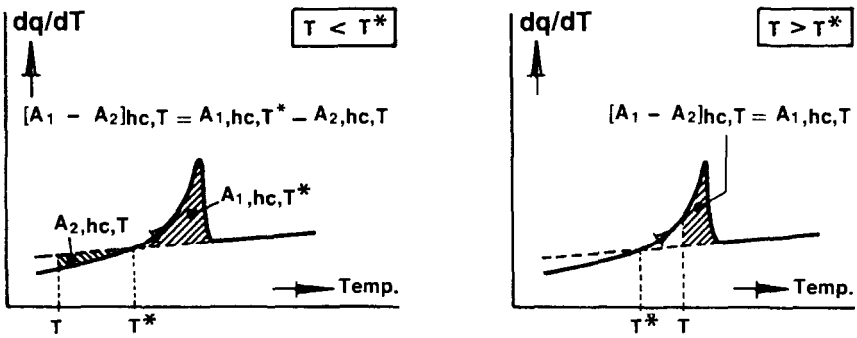

Fig. 3. Some definitions for a heating curve in order to calculate crystallinity at T by extrapolation from the melt; similar definitions apply to a cooling curve.

There is a third phase - occurring very often in some polymers and only occasionally in others, depending on their history - which is called the 'rigid amorphous' phase. It is assumed that in this phase, because of limited mobility of the molecules in it, a portion of the material, and particularly the crystalline-amorphous transition layer, still has a glass character far above the normal glass transition. Because of this the c_p of this non-crystalline material is better approximated by $c_{p_g} \approx c_{p_c}$ than by c_{p_a}. The extent to which the two-phase model is then still applicable is a subject of study [11-13]. For the samples discussed here it is not possible, on the basis of DSC measurements alone, to evaluate the presence of such a third phase, for one thing because in the case of polymers with ethylene crystallinity glass transition phenomena are hardly measurable, if at all, making the necessary Δc_p (T_g) evaluation impossible.

Within the two-phase model, the crystallinity is usually obtained by dividing $A_{1,hc,T*}$ by the theoretical value of the heat of fusion of the polymer, $\Delta h(T_m)$. For polyethylene, normally $\Delta h(414.6\ K) = 293\ J/g$ is used [8], taking $T_m = 414.6\ K$ as theoretical melting point.

However, a crystallinity determination in such a way is known to be inadequate (see [4] and references therein), and thus forms a shaky basis. One should be well aware of this when comparing DSC results with results reached using other techniques or when using DSC results for calculation of a rigid amorphous fraction.

Firstly, the value thus obtained is dependent on T*, and hence on the shape of the curve. Secondly, instead of $\Delta h(T_m)$, the value $\Delta h(T^*)$ should be used.

It can be proved that the correct value of the weight percentage crystallinity $W^c(T)$ can be obtained at any desired temperature (above, at or below T*) if $c_{p_a}(T)$ is sufficiently accurately approximated by the curve resulting from an extrapolation from the melt and if the temperature dependence of Δh is taken into account. On this basis, see Fig. 4, $W^c{}_{hc}(T)$ and $W^c{}_{cc}(T)$ have been calculated for the linear polyethylene [4] NBS SRM 1484 [M_n = 91, M_w = 121, M_z = 154 (kg/mol)] using the following formula (for definition of $[A_1 - A_2]_T$, see Fig. 3):

$$W^c(T) = \frac{[A_1 - A_2]_T}{\Delta h(T)_M} * 100\ \% \qquad (1)$$

with

$$\Delta h(T)_M = 293 - 0.3092*10^{-5}(414.6 - T)^2(414.6 + 2T)\ J/g \qquad (2)$$

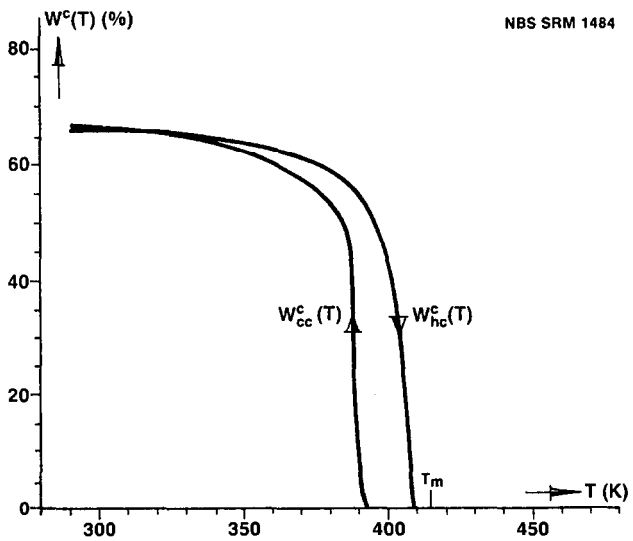

Fig. 4. Weight percentage crystallinity above 290 K for the linear polyethylene NBS SRM 1484 in cooling from 473 K to 203 K at 10 K/min, $W^c{}_{cc}(T)$, and heating at 10 K/min, $W^c{}_{hc}(T)$. Sample mass 4.320 mg.

which function can be used for T > 290 K [8]. The actual measurements spanned 270 degrees, from 203 K to 473 K.

The method can be used for ordinary and heat capacity DSC cooling and heating curves, even if there is no point of intersection (this situation is to be treated as T > T*).

CRYSTALLINITY FROM DSC HEAT CAPACITY CURVES

The above-described method of determining the crystallinity is based on determination of the enthalpy-based weight percentage crystallinity, which is defined by

$$w^c(T) = \frac{h_a(T) - h(T)}{h_a(T) - h_c(T)} \cdot 100\ \% \qquad (3)$$

where h(T) is calculated from the experimental heat capacity curve, while the reference values $h_a(T)$ and $h_c(T)$ for purely amorphous and purely crystalline polyethylene are obtained via integration of $c_{p_a}(T)$ and $c_{p_c}(T)$, respectively, see Table 4, ref. 8, and [4].

This procedure is illustrated by presenting heat capacity measurements of a (linear) Ultra-High Molecular Weight Polyethylene (Hifax 1900: UHMWPE with M_w = 3200 kg/mol, M_w/M_n = 4), see Fig. 5. The material used was a reactor powder that had never been melted before.

The first heating curve shows melting behaviour at very high temperatures: it should be borne in mind that an important part of the curve lies above the theoretical melting point T_m = 141.4 °C. A rough estimate of the peak area already suggests a large heat of fusion. The high melting temperatures are caused by a combination of factors.

First of all, the thermal conductivity within the pill prepared by very gentle compression of the powder is poor. The pill had to be made in view of the high sample mass of 11.106 mg. Sample mass has a big influence; with a mass of 11.106 mg, the top temperature is 146 °C at a heating rate (S_h) of 10 °C/min, whereas 143 °C is found with a sample mass of 0.871 mg despite the higher S_h = 20 °C/min. With a low sample mass of about 0.8 mg, the powder grains are spread across the pan and heat conduction is no problem. Incidentally, lowering the scanning rate also lowers the top temperature, albeit to a lesser degree: 143 °C (S_h = 20 °C/min); 141.5 °C/min (S_h = 5 °C/min) to 141 °C (S_h = 1.25 °C/min) with sample sizes of between 0.803 and 0.871 mg.

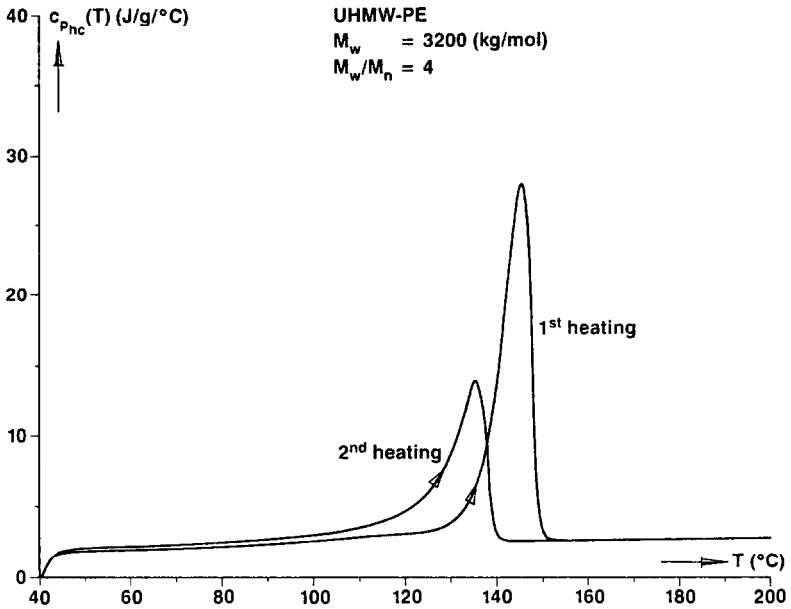

Fig. 5. DSC-2 specific heat capacity curves for a UHMWPE from 1st heating run to 200 °C, and 2nd heating run to the same temperature after cooling to 40 °C. Scanning rate 10 °C/min, sample mass 11.106 mg.

Another cause of the high melting temperatures is superheating of the fairly perfect crystals in the reactor powder created during polymerization.

The phenomena found must not be confused with the solid -> solid transition from orthorhombic to hexagonal which appears around 155 °C when constraints are placed upon the material [14].

The reason for the choice of the measuring conditions named was the wish, in this specific case, to measure the c_p's quantitatively at lower temperatures so that any pre-melting would become clearly visible and, furthermore, to arrive in this way at a reliable determination of crystallinity as a function of the temperature between 40 °C and about 120 °C. It can be clearly seen from the c_p curves that melting already occurs at low temperatures, since at such temperatures the heat capacities lie above the curve obtained by means of extrapolation from the melt, which curve - as remarked earlier - is a good approximation of $c_{p_a}(T)$. Apparently, along with the fairly perfect crystals mentioned above, relatively unstable crystals are also present. In determining the heat of fusion, this pre-melting must, of course, be taken seriously and the earlier discussion regarding peak evaluation applies.

It is important to note that the state of the reactor powder - created out of the unique combination of polymerization and crystallization - is influenced irreversibly by melting [15]. After an isothermal waiting time at 200 °C of 5 minutes and subsequent cooling to 40 °C, the second heating curve was measured, showing a normal picture of the melting of a high molecular weight linear polyethylene (under the selected measuring conditions).

In Fig. 6, the $h_{hc}(T)$ curves of the UHMWPE from Fig. 5 are shown besides the reference curves $h_a(T)$ and $h_c(T)$. The $h_{hc}(T)$ curves were obtained by numerical integration of the $c_{p_{hc}}$ values. For the second heating curve, the calibration with respect to $h_a(T)$ was performed as usual at (141.4 °C, 779 J/g), see Table 4, ref. 8. In the case of the first heating curve, the superheating mentioned creates a slight complication. Calibration with respect to $h_a(T)$ was performed at 155 °C whereas $h_c(T)$ was obtained at between 141.4 °C and 155 °C (see the broken line in the figure) by integration of the

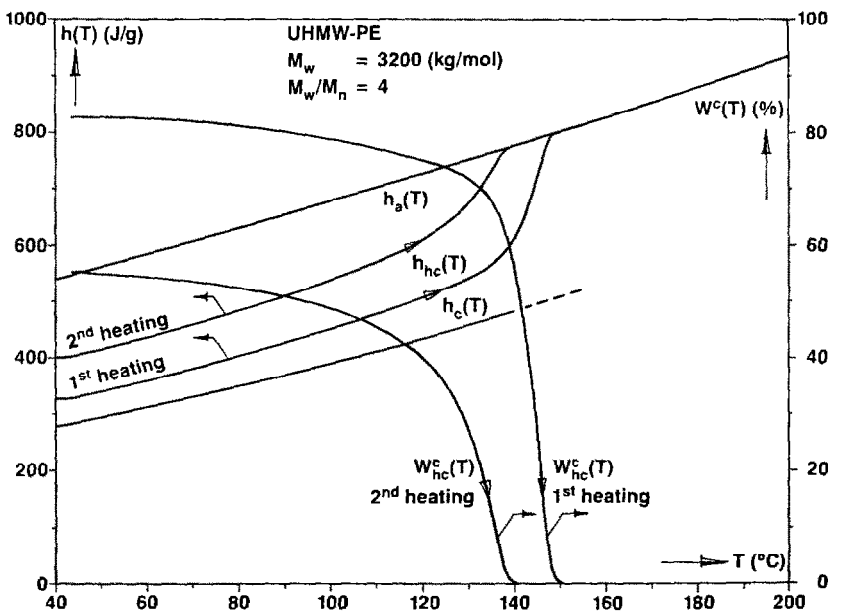

Fig. 6. Specific enthalpy heating curves, $h_{hc}(T)$, for a UHMWPE based on measurements shown in Fig. 5, the reference curves for purely amorphous polyethylene, $h_a(T)$, and purely crystalline polyethylene, $h_c(T)$, and the enthalpy-based weight percentage crystallinity heating curves, $W^c_{hc}(T)$.

extrapolated $c_{p_c}(T)$ function in that region. With the help of these data, $W^c_{hc}(T)$ was calculated for both heating curves in the temperature range of the measurement.

Crystallinities at 40 °C for the UHMWPE reactor powder and for the UHMWPE after crystallization at a cooling rate of 10 °C/min amount to 83 % and 55 %, respectively. A decline in W^c is clearly seen from 40 °C onwards, especially during the second heating run. For recrystallized UHMWPE, clarity about the effect of any rigid amorphous phase present would be useful; evidence concerning it can be found, for example, in three-component analyses of the broad-line proton NMR spectrum for linear polyethylenes [16].

As an extreme example, the value W^c for an octene-1 VLDPE (Very Low Density Polyethylene; VLDPE densities are lower than about 915 kg/m^3; in the figures X_8 denotes the mole percentage octene) as a function of the temperature will be calculated. VLDPEs are heterogeneous ethylene copolymers which, see Fig. 7, show extremely wide crystallization and melting ranges, typically

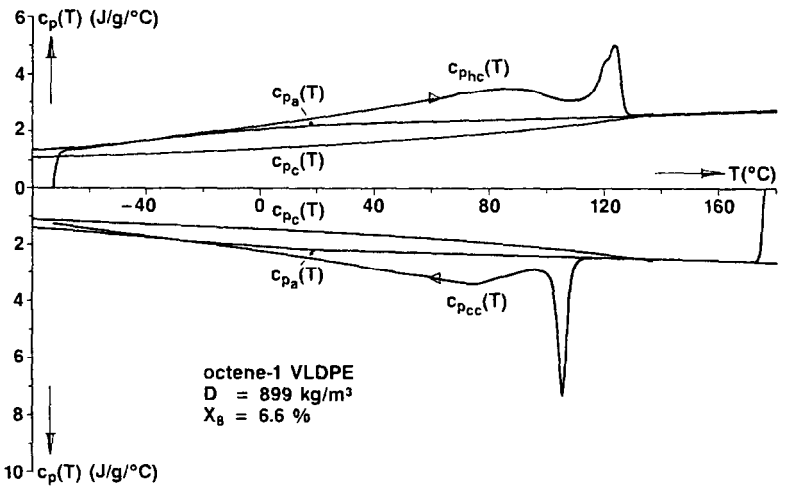

Fig. 7. DSC-2 specific heat capacity curves for cooling, $c_{p_{pc}}(T)$, at 10 °C/min from 177 °C to -73 °C and subsequent heating, $c_{p_{phc}}(T)$, at 10 °C/min for a VLDPE (7.321 mg). Reference curves for purely amorphous polyethylene, $c_{p_a}(T)$, and purely crystalline polyethylene, $c_{p_c}(T)$.

covering about 200 degrees [17-19]. In the melt, the $c_p(T)$ for the VLDPE studied is in close agreement with $c_{p_a}(T)$, while only at the lowest temperatures the $c_p(T)$ curves lie between the $c_{p_c}(T)$ curve and the $c_{p_a}(T)$ curve, indicating that there is virtually no crystallization or melting.

The figure further shows that over a wide temperature range $c_{p_a}(T)$ is approximated well by extrapolation from the melt but that below 290 K the c_{p_a} function shows a sharper drop with decreasing temperature than would have been

expected on the basis of the extrapolation, eventually arriving at the same value as the c_{p_c} function at about 120 K [8].

There are good reasons to assume that the two-phase model is applicable to octene-1 VLDPE, in the sense that a well-defined amorphous phase and crystalline phase are present, which means that the quantity $W^c(T)$ may be identified with the enthalpy-based weight crystallinity. After all, under the plausible assumption that, considering the length of the comonomer octene-1, the majority of the octene groups are excluded from the crystal lattice [1,13,20,21], we may assume that the crystalline phase is well-defined.

In Fig. 8, the $h_{hc}(T)$ curve of the VLDPE from Fig. 7 is shown besides the reference curves $h_a(T)$ and $h_c(T)$. The value $W^c{}_{hc}(T)$ was calculated as

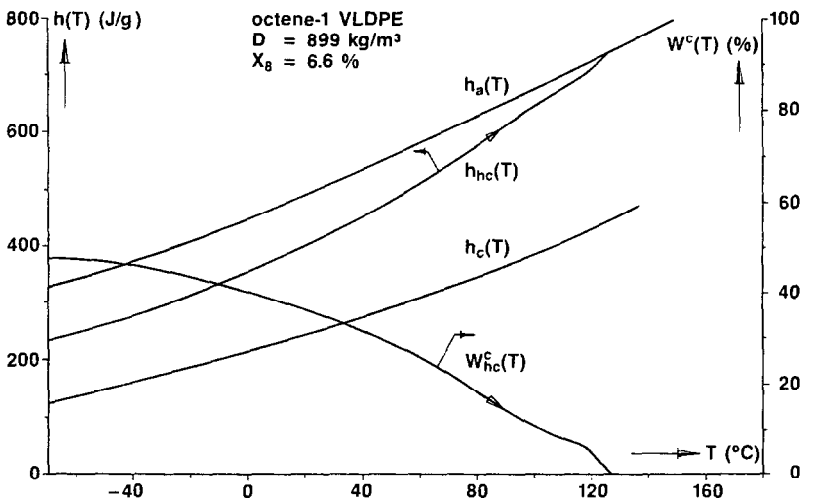

Fig. 8. Specific enthalpy heating curve, $h_{hc}(T)$, for a VLDPE based on measurements shown in Fig. 7, the reference curves for purely amorphous polyethylene, $h_a(T)$, and purely crystalline polyethylene, $h_c(T)$, and the enthalpy-based weight percentage crystallinity heating curve, $W^c{}_{hc}(T)$.

indicated before for the temperature range of the measurement. It shows that the melting process is already in progress from -60 °C onwards and is not finished until about 130 °C. The crystallinity at 23 °C, which is 36 %, is considerably lower than that at -60 °C, which is 48 %. This is in good agreement with the values for a VLDPE [19] with the same density at room temperature.

PEAK BASE LINE AND EXCESS HEAT CAPACITY

With the help of the data above it is possible, for most crystallizable polymers, to define a meaningful base line for crystallization and melting peaks. The starting point of this definition is that integration of the measured heat capacity, $c_p(T)$, leads directly to an h(T) without the need to assume a model regarding the phenomenon to be investigated. In the case of crystallization and melting an absolute enthalpy function is obtained through calibration with respect to $h_a(T_m)$.

Assumption of a model only becomes relevant when it comes to interpretation. Within the most simple - and nonetheless very useful - two-phase model for polymers, the specific heat capacity measured can be described as the sum of two terms, viz. a base-line term and an excess term: differentiation of h(T) in the expression within the two-phase model for the enthalpy-based weight fraction crystallinity, $w^c(T)$, yields

$$c_p(T) = \underbrace{[1 - w^c(T)]*c_{p_a}(T) + w^c(T)*c_{p_c}(T)}_{\{\text{meas. } c_p\} = \{\text{base-line } c_p\}} \underbrace{- [h_a(T) - h_c(T)]*dw^c(T)/dT}_{+ \{\text{excess } c_p\}} \qquad (4)$$

or

$$c_p(T) = c_{p_b}(T) + c_{p_e}(T) \qquad (5)$$

The first term, here called base-line c_p, is nothing other than the c_p of a semi-crystalline polymer based on additivity of the c_p contributions of the amorphous and crystalline phases. That is also the only contribution if the last term, here called excess c_p, can be neglected - if there is no change in crystallinity, for example [22]. Extrapolation from experimental c_p's to 100 % amorphous and 100 % crystalline according to crystallinity with the objective of determining, respectively, c_{p_a} and c_{p_c}, rests on such an assumption, as does determination of crystallinity in the glass transition region from $c_p(T_g)$ using $c_{p_a}(T_g)$ and $c_{p_c}(T_g)$.

Fig. 9 plots the base-line c_p for the heating curve, $c_{p_{b,hc}}(T)$, for the VLDPE in addition to the curves shown in Fig. 7. The measurement was performed on a fresh sample and, compared to the measurement shown in Fig. 7, is of somewhat lesser quality - as appears from the systematic deviation in the melt part range with regard to $c_{p_a}(T)$. Fig. 10 shows the excess c_p for the heating curve, $c_{p_{e,hc}}(T)$. In the melt $c_{p_e} = c_p - c_{p_a}$ because $w^c = 0$. In this particular case, c_{p_e} is visibly unequal to zero because of the just-mentioned systematic deviation of c_p with respect to c_{p_a}.

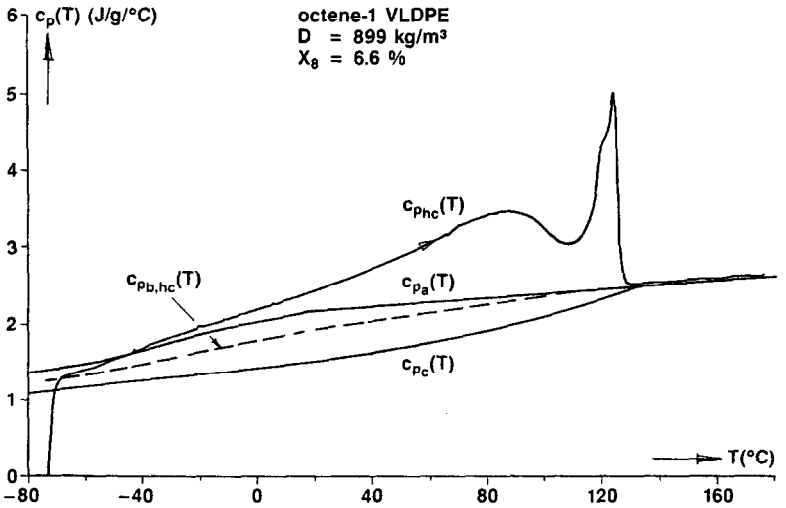

Fig. 9. DSC-2 specific heat capacity curves for heating, $c_{p_{hc}}(T)$, at 10 °C/min for a VLDPE (10.768 mg) after cooling at 10 °C/min from 177 °C to -73 °C. Reference curves for purely amorphous polyethylene, $c_{p_a}(T)$, and purely crystalline polyethylene, $c_{p_c}(T)$. Broken curve: base-line c_p for the heating curve, $c_{p_{b,hc}}(T)$.

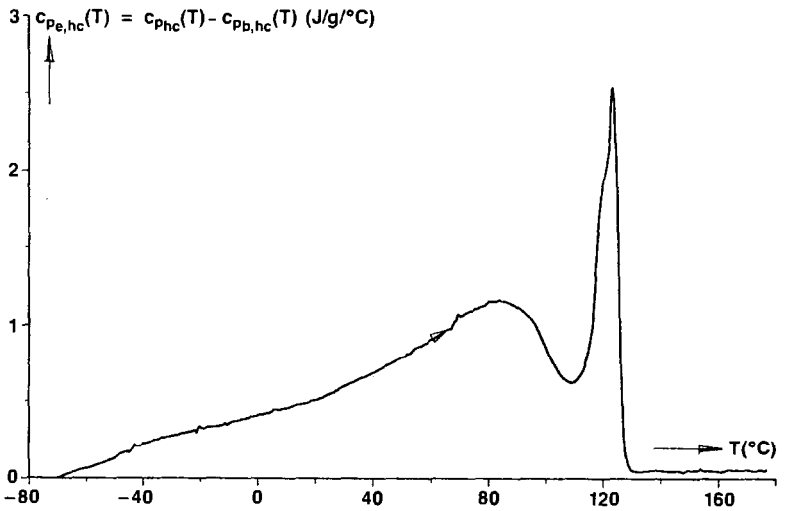

Fig. 10. The excess-c_p for the heating curve, $c_{p_{e,hc}}(T)$, for a VLDPE based on the measurement shown in Fig. 9.

The outlined method clearly distinguishes between, on the one hand, the contribution of the temperature-dependent c_{p_a} and c_{p_c} for, respectively, the amorphous and crystalline phases in the experimental cp through crystallinity and, on the other, the contribution of the melting in the experimental c_p. The same evaluation can be made, of course, for cooling and concomitant crystallization.

A c_p measurement need not necessarily be made in calculating $c_p(T)_{excess}$:

$$c_p(T)_{excess} = [h_a(T) - h_c(T)]*dw^c(T)/dT \qquad (6)$$

The enthalpy differential function $h_a(T) - h_c(T) = \Delta h(T)$ is known for many polymers. For polymers with ethylene crystallinity this function can in actual practice be excellently approximated above 290 K by the function $\Delta h(T)_M$ mentioned earlier. If the temperature dependence of the function is not known, one is forced to use a constant value, for which the best estimate will be $\Delta h(T)_M$. The change in crystallinity with temperature, $dw^c(T)/dT$, can be numerically calculated from $w^c(T)$. The latter can be calculated, in the way shown earlier, from an ordinary DSC curve.

All this also means that the base line for a dq/dT measurement of a polymer can be calculated according to

$$\begin{aligned}(dq/dT)_{base} &= (dq/dT)_{meas.} - (dq/dT)_{excess} \\ &= (dq/dT)_{meas.} - c_p(T)_{excess}\end{aligned} \qquad (7)$$

As stated earlier, this procedure is only meaningful if the measurement is quantitative in the sense that simple extrapolation from the melt is meaningful when determining $w^c(T)$. This implies the supposition that the instrumental component in $(dq/dT)_{base}$ must be only linearly dependent on the temperature.

$$(dq/dT)_{base} = c_{p_b}(T) + C1 + C2*T \qquad (8)$$

Using the method above, good results can be achieved if an empty pan measurement is standardly subtracted from the actual measurement. One thus corrects for temperature-dependent instrumental deviations, one and the same empty pan measurement normally being usable for several measurements and sometimes - depending on the stability of the DSC and possible fouling by the sample - for several days or longer. The 'pseudo c_p' character of such measurements makes it possible to obtain more insight into the quality of a measurement, because one can make comparisons with reference states and, in particular, check the temperature dependence. Simple checks are $dc_{p_s}(T)/dT$,

$dc_{p_l}(T)/dT > 0$; $dc_{p_s}(T)/dT > dc_{p_l}(T)/dT$, etc. In actual practice, however, it is recommendable to avoid confusion with a real c_p measurement by standardizing the presentation of such 'pseudo c_p' measurements by, for example, plotting the curves horizontally. This means making the curve part that represents the signal from the melt temperature-independent by adding to the measured signal a linearly temperature-dependent component. It will be clear that none of this will interfere with the earlier-described procedure for determining $c_p(T)_{excess}$ and $(dq/dT)_{base}$. It is further recommendable not to specify a c_p axis with an absolute scale in pseudo c_p measurements.

REFERENCES

1 B. Wunderlich, Macromolecular Physics, Vols. 1 (1973), 2 (1976) and 3 (1980), Academic Press, New York.

2 M.J. Richardson, in J.V. Dawkins (Ed.). Developments in Polymer Characterization, Vol. 1, Applied Science Publishers Ltd, London. 1978, p. 205.

3. U. Gaur, H-C. Shu, A. Mehta and B. Wunderlich, J. Phys. Ref. Data, 10 (1981) 89.

4 V.B.F. Mathot and M.F.J. Pijpers, J. Therm. Anal., 28 (1983) 349.

5 V. Mathot, M. Pijpers, J. Beulen, R. Graff and G. van der Velden, in D. Dollimore (Ed.). Proceedings of the Second European Symposium on Thermal Analysis 1981 (ESTA-2), Heyden, London, 1981, p. 264.

6 V.B.F. Mathot, H.M. Schoffeleers, A.M.G. Brands and M.F.J. Pijpers, in B. Sedláček (Ed.). Morphology of Polymers, Walter de Gruyter & Co., Berlin - New York, 1986, p. 363.

7 V.B.F. Mathot, Ch.C.M. Fabrie, G.P.J.M. Tiemersma-Thoone and G.P.M. van der Velden. Proceedings Int. Rubber Conf., Kyoto, October 15-18, 1985, p. 334.

8 V.B.F. Mathot, Polymer, 25 (1984) 579.

9 K. Loufakis and B. Wunderlich, J. Phys. Chem., 92 (1988) 4205.

10 B. Wunderlich and S.Z.D. Cheng, Gazzetta Chimica Italiana, 116 (1986) 345. B. Wunderlich, Un. of Tennessee, The fifth ATHAS report (1989)

11 S.-D. Clas, R.D. Heyding, D.C. McFaddin, K.E. Russell, M.V. Scammell-Bullock, E.C. Kelusky and D.St-Cyr, J. Polym. Sci. Polym. Phys., 26 (1988) 1271.

12 S.Z.D. Cheng and B. Wunderlich, Thermochim. Acta, 134 (1988) 161.

13 R.G. Alamo and L. Mandelkern, Macromolecules, 22 (1989) 1273.

14 N.A.J.M. van Aerle and P.J. Lemstra, Polym. J. 20 (1988) 131.

15 P. Smith, H.D. Chanzy and B.P. Rotzinger, J. Mater. Sci., 22 (1987) 523.

16 R. Kitamaru and F. Horii, Adv. Polym. Sci., 26 (1978) 139.

17 V.B.F. Mathot and M.F.J. Pijpers, in P.J. Lemstra and L.A. Kleintjens (Eds.). Integration of Fundamental Polymer Science and Technology 1987, Elsevier Applied Science Publishers Limited, London, England, Vol. 2, 1988, p. 381. V.B.F. Mathot, R.A.C. Deblieck and M.F.J. Pijpers, in P.J. Lemstra and L.A. Kleintjens (Eds.). Integration of Fundamental Polymer Science and Technology 1988, Elsevier Applied Science Publishers Limited, London, England, Vol. 3, 1989, p. 287.

18 R.A.C. Deblieck and V.B.F. Mathot, J. Mater. Sci. 7 (1988) 1276.

19 V.B.F. Mathot and M.F.J. Pijpers, J. Appl. Polym. Sci., in press.

20 R. Seguela and F. Rietsch, J. Polym. Sci., Polym. Letters Ed., 24 (1986) 29.

21 C. France, P.J. Hendra, W.F. Maddams and H.A. Willis, Polymer, 28 (1987) 710.

22 M. Dole, J. Polym. Sci, Part C, 18 (1967) 57.